Mongolian Journal of Agricultural Sciences, Vol.17, No.41 (2024)
https://doi.org/10.5564/mjas.v17i41.1466

Differential Transcriptomic Analysis of *Glutamicibacter arilaitensis* Under Varying Culture Temperatures

Xu Chun-guang[1]*, Yang Li-xia[1], Wang Ji-chun[1], Ma Yu-jiao[1] and Yu Bao-li[2]

[1]College of Agriculture, Hulunbuir University，No. 26, Middle Road, Genghis Khan, Hailar District, Hulunbuir City, Inner Mongolia Autonomous Region, 021008, China
[2]Hulunbuir Agricultural and Animal Husbandry Technology Promotion Center，Hulunbuir, Inner Mongolia, 021000, China

*Corresponding author: 418380078@qq.com

https://orcid.org/0009-0008-4533-4940

Received: 18.06.2024 Revised: 15.11.2024 Accepted: 01.12.2024

Abstract

Low-temperature adaptation is a critical physiological process in mesophilic bacteria, yet its molecular mechanisms remain unclear. To investigate how *Glutamicibacter arilaitensis* strain F9 adapts to cold stress, the strain was cultured at 5°C (F9_5), 10°C (F9_10), and 25°C (F9_25). High-throughput transcriptome sequencing was performed to analyze differentially expressed genes (DEGs) across these conditions. Gene expression differences were identified and subjected to Gene Ontology (GO) enrichment and Kyoto Encyclopedia of Genes and Genomes (KEGG) pathway analyses.

A total of 731 DEGs were identified between F9_25 and F9_10, 747 between F9_25 and F9_5, and 265 between F9_10 and F9_5, with 65 shared DEGs across all comparisons. GO enrichment analysis revealed associations primarily with cellular energy metabolism, amino acid biosynthesis, and membrane components. KEGG pathway analysis identified 20 significantly enriched pathways. Key differences included dicarboxylate metabolism, ABC transporters, and two-component systems (F9_25 vs. F9_10); two-component systems, pyruvate metabolism, and glyoxylate/dicarboxylate metabolism (F9_25 vs. F9_5); and fatty acid degradation and tryptophan metabolism (F9_10 vs. F9_5).

To survive low-temperature stress, strain F9 modulated gene expression to counteract the reduction in enzyme activity and protein efficiency. This regulation helped maintain membrane fluidity and ensured proper substance exchange and signal transduction, while also securing sufficient energy and biosynthetic precursors for essential cellular functions.

Keywords: transcriptome analysis; GO enrichment analysis; KEGG; psychrophilic mechanism

Introduction

Cold resistance mechanisms of bacteria are primarily concentrated on several aspects, including the structure and composition of the cell membrane, structural characteristics of tRNA, kinetic structure of enzymes, and antifreeze proteins [1], [2]. Mesophilic bacteria have lower membrane lipid content and fewer straight-chain and branched unsaturated fatty acids than psychrophilic bacteria, leading to a higher lipid melting point. As a result, their membrane fluidity decreases under low temperatures, limiting their adaptation to cold environments [3]. Transcriptomic profiling is a powerful tool for annotating gene functions and regulatory architectures [4]. By systematically analyzing transcriptional landscapes, including alternative splicing events, tissue-specific isoforms, and microRNA-target interactions, it provides critical insights into cellular regulatory networks and molecular mechanisms underlying physiological processes [5], [6]. To investigate the molecular basis of cryotolerance in *Glutamicibacter arilaitensis* F9, a multi-temperature transcriptomic approach was employed at 5°C, 10°C, and 25°C. RNA sequencing was performed using the Illumina NovaSeq platform, and differential expression analysis was conducted with DESeq2, applying a false discovery rate (FDR) threshold of ≤0.05. Identified differentially expressed genes (DEGs) were further analyzed using GO Slim and KEGG Orthology annotation to identify key genes associated with membrane fluidity regulation and cold-shock response pathways [7], [8].

Materials and Methods

Bacterial Strain and Cultivation

Glutamicibacter arilaitensis strain F9 was isolated from agricultural soil collected in April 2019 at Guribanhua Suomu, Naiman Banner, Inner Mongolia (42.1234°N, 119.2345°E). The taxonomic identity was confirmed through 16S rRNA gene sequencing using primers 27F/1492R. BLAST alignment revealed 99.8% sequence similarity with *G. arilaitensis* strain Re117 (GenBank accession: MK424282.1), confirming strain-level identity [3]. Cellulolytic activity was verified using low-temperature cellulase assays, confirming the psychrotrophic nature of the isolate.

Culture Conditions and Sample Preparation

Strain F9 was streaked on LB agar and incubated at 10°C for 3–4 days to form visible colonies. Single colonies were transferred to LB liquid medium and diluted 1:100 (v/v) into fresh broth. The cultures were grown under shaking conditions (110 rpm) at three temperatures—5°C (cold stress), 10°C (moderate cold), and 25°C (optimal)—until reaching the early exponential phase (OD600 = 0.6–0.8). Cells were harvested by centrifugation at 12,000 rpm for 3 min at 4°C, flash-frozen in liquid nitrogen, and stored at −80°C. Each temperature group consisted of four biological replicates [4].

RNA Extraction and Transcriptome Sequencing

Total RNA was extracted using the TRIzol® reagent kit (Thermo Fisher Scientific) according to the manufacturer's instructions. Purity and concentration were measured with a Nanodrop 2000 (Thermo Fisher), and integrity was evaluated using agarose gel electrophoresis and an Agilent 2100 Bioanalyzer (Agilent Technologies). Ribosomal RNA was removed prior to fragmentation. First-strand cDNA synthesis was carried out with random hexamer primers, followed by second-strand synthesis, end repair, poly-A tailing, adaptor ligation, and PCR enrichment. Libraries were sequenced on an Illumina NovaSeq platform (Wuhan Feisha Gene Technology Co., Ltd.) [5].

Transcriptome Analysis and Reference Mapping

Raw reads underwent quality filtering using SOAPnuke to remove low-quality bases, adapter sequences, and short fragments (<20 bp). Clean reads were aligned to the reference genome of *G. arilaitensis* Re117 (GenBank accession: PRJEA50353) using BWA within the SOAP2.2.1 package with default parameters [6]. Mapping metrics included alignment rates, read uniqueness, exon-intron junction coverage, and sequence identity percentage.

Differential Gene Expression Analysis

Gene expression levels were normalized using the RPKM (Reads Per Kilobase per Million mapped reads) method. Differentially expressed genes (DEGs) were identified with the edgeR package in R, using FDR < 0.05 and |log2 fold change| > 1 as thresholds for significance [7].

Gene Ontology (GO) and KEGG Pathway Enrichment

GO term enrichment was calculated using hypergeometric distribution, with p-values adjusted by the Benjamini-Hochberg method to control FDR. KEGG pathway enrichment analysis was performed using annotated gene sets and plotted using clusterProfiler in R. Enrichment was considered significant at FDR ≤ 0.05 [8].

Statistical Analysis

All statistical analyses were conducted in R version 3.6.1. Differences between groups were evaluated by one-way ANOVA followed by Tukey's post hoc test. Significance was set at $p < 0.05$ unless otherwise stated.

Results

Genome Sequence Alignment of *Glutamicibacter arilaitensis* F9 and Reference Strain

To assess the transcript alignment efficiency, high-quality reads from *G. arilaitensis* F9 cultivated at 5°C, 10°C, and 25°C were mapped to the reference genome of *G. arilaitensis* Re117. Table 1 presents a summary of alignment metrics, including total mapped reads, perfect matches, and uniquely mapped reads across biological replicates. Mapping efficiency ranged from 60.29% to 87.36%, indicating high data quality and strong correspondence with the reference genome [6]. The unique mapping rate exceeded 70% in most samples, and mismatches were typically below 5 bp, validating the suitability of these transcriptomes for differential expression analysis.

Table 1.

Read alignment summary for each sample across three temperature conditions (F9_5, F9_10, F9_25)

Sample	Total Reads	Total Mapped (%)	Perfect Matches (%)	≤5bp Mismatch (%)	Unique Mapped (%)	Multiple Mapped (%)
F9_1_5	8,167,350	78.16	30.34	47.15	65.67	12.49
F9_3_5	13,093,290	87.36	37.49	49.21	84.53	2.83
F9_4_5	17,945,650	83.81	35.45	47.75	79.79	4.02
F9_1_10	9,433,680	81.03	35.19	45.25	74.15	6.88
F9_2_10	10,821,640	81.98	37.09	44.33	75.19	6.79
F9_3_10	11,229,046	81.16	35.25	45.29	74.97	6.19
F9_1_25	46,295,936	61.20	30.40	30.43	58.25	2.94
F9_2_25	17,207,142	60.29	25.00	34.78	55.93	4.36
F9_3_25	10,812,940	77.64	37.81	39.31	73.62	4.02

Principal Component and Correlation Analysis

Principal component analysis (PCA) was conducted to assess transcriptomic variation among G. arilaitensis F9 samples cultured at 5°C, 10°C, and 25°C. The analysis revealed strong intra-group consistency and clear separation between temperature conditions, indicating temperature-dependent transcriptional profiles (Figure 1). The first two principal components explained 77.7% of the total variance, confirming the quality of the data and supporting its suitability for downstream differential expression analysis.

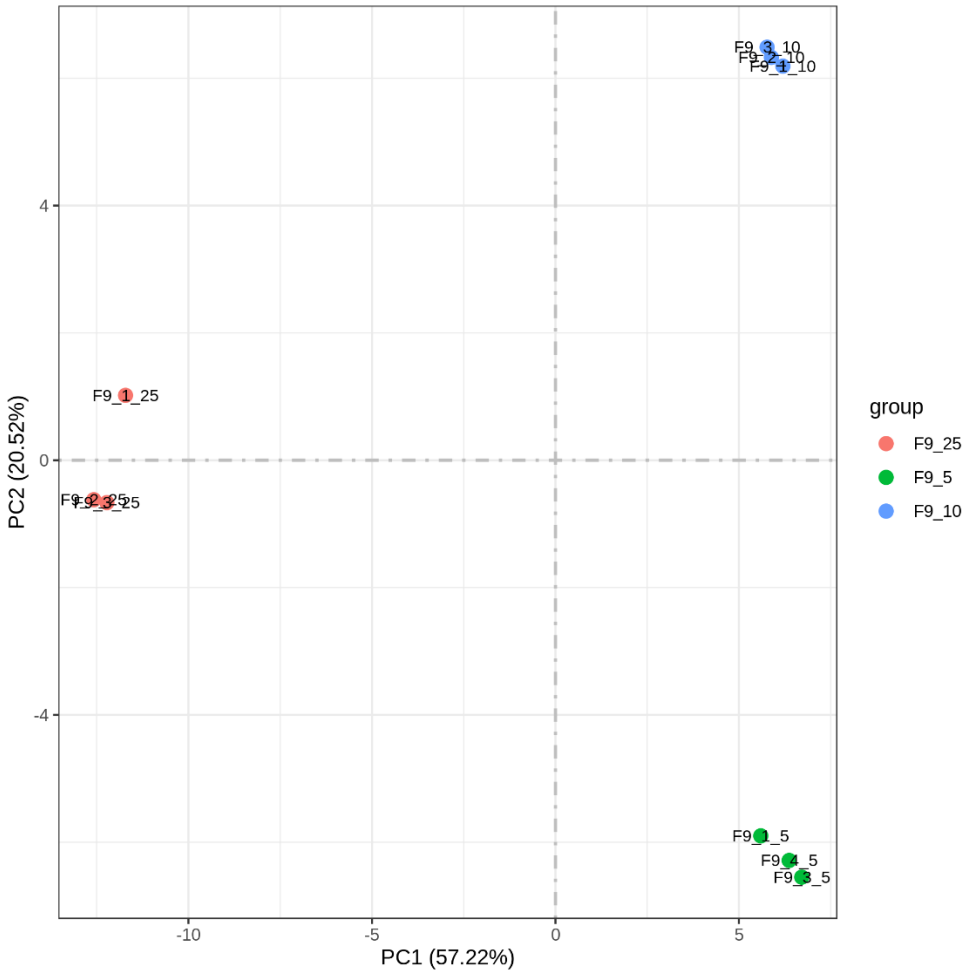

Figure 1. PCA plot of gene expression across all samples.

Heatmap analysis (Figure 2) supported the PCA results by illustrating strong sample-to-sample correlation. Intra-group coherence was high, with average correlation coefficients exceeding 0.98 across all replicates, indicating minimal technical variation. Inter-group comparisons revealed that samples at 5°C and 10°C were highly similar (correlation >0.96), likely reflecting shared cold-adaptive transcriptional responses. In contrast, samples cultured at 25°C showed lower correlation (<0.92) with those at lower temperatures, consistent with previous observations of transcriptional divergence in psychrophilic organisms exposed to non-optimal, warmer conditions. This pattern highlights temperature-dependent regulation of key metabolic genes in *Glutamicibacter arilaitensis* F9, particularly those associated with glycolysis, amino acid biosynthesis, and membrane fluidity.

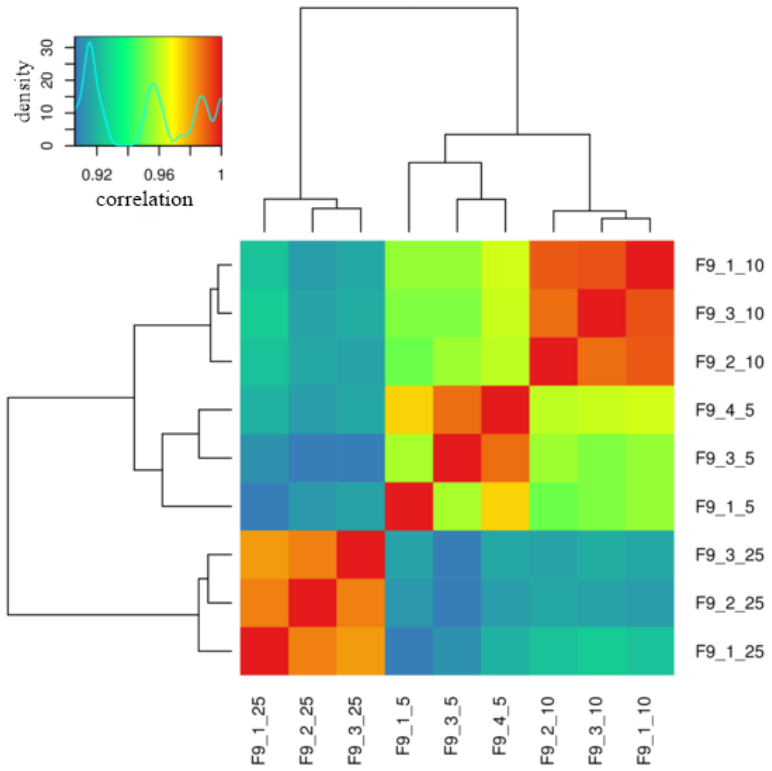

Figure 2. Heatmap of sample correlation coefficients.

Identification of Differentially Expressed Genes

Differential gene expression analysis was conducted to compare transcriptomic profiles of *Glutamicibacter arilaitensis* F9 cultured at three temperatures: 5 °C, 10 °C, and 25 °C. The pairwise comparisons included F9_25 vs. F9_10, F9_25 vs. F9_5, and F9_10 vs. F9_5. The results, summarized in Table 2, revealed that the F9_25 vs. F9_10 group exhibited the highest number of downregulated genes (424), while the F9_25 vs. F9_5 group had the highest number of upregulated genes (334). The F9_10 vs. F9_5 comparison showed the fewest differentially expressed genes, with 147 upregulated and 118 downregulated, suggesting limited transcriptional divergence between these two closely related cold-temperature conditions.

Table 2.

Summary of differentially expressed genes (DEGs) (FDR < 0.05, $|\log_2 FC| > 1$)

Group Comparison	Total DEGs	Upregulated	Downregulated
F9_25 vs. F9_10	731	307	424
F9_25 vs. F9_5	747	334	413
F9_10 vs. F9_5	265	147	118

Overlap and Distribution of Differentially Expressed Genes

A Venn diagram (Figure 3) was constructed to visualize the overlap of DEGs among the three pairwise comparisons. A total of 65 DEGs were common to all three comparisons, suggesting that these genes may play a core role in temperature adaptation in *G. arilaitensis* F9. The largest overlap was observed between the F9_25 vs. F9_10 and F9_25 vs. F9_5 groups, with 488 shared DEGs, indicating a strong response to the temperature shift from 25 °C to lower temperatures. In contrast, the F9_10 vs. F9_5 group had only 45 unique DEGs, supporting the notion that transcriptomic changes between 5 °C and 10 °C are relatively modest, likely due to similar cold-adaptive physiological states under these conditions.

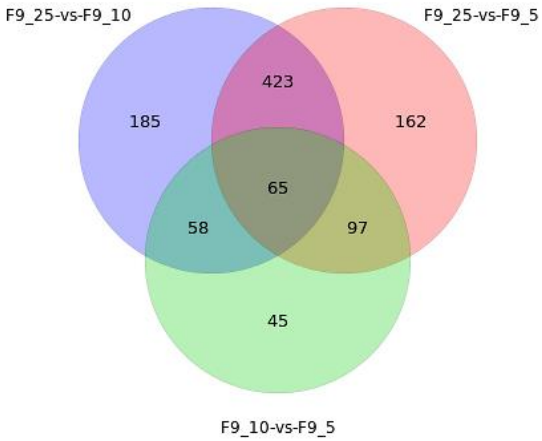

Figure 3. Venn diagram showing overlapping differentially expressed genes across the three temperature comparison groups.

Volcano Plot Analysis

Volcano plots (Figure 4) provide a visual representation of differentially expressed genes (DEGs) by displaying statistical significance (false discovery rate, FDR) against the magnitude of expression change (fold change, FC) for each gene across pairwise comparisons. This approach enables simultaneous evaluation of both the biological relevance and statistical reliability of gene expression differences. In the F9_25 vs. F9_5 comparison, the largest number of significantly upregulated and downregulated genes was observed, indicating substantial transcriptional divergence between ambient temperature (25 °C) and cold conditions (5 °C). The F9_25 vs. F9_10 comparison exhibited an intermediate number of DEGs, reflecting a moderate transcriptomic shift. In contrast, the F9_10 vs. F9_5 group showed the fewest DEGs, suggesting minimal transcriptional changes between these two closely related low-temperature conditions. These results indicate that culturing *Glutamicibacter arilaitensis* F9 at 25 °C triggers extensive metabolic reprogramming compared to cold environments, likely due to the activation of stress-responsive pathways including genes involved in membrane fluidity, protein folding, and cold-shock adaptation. Conversely, the limited differences observed between the 10 °C and 5 °C treatments imply functional redundancy in gene expression under mild thermal variation, where small temperature changes may not substantially impact regulatory networks or cellular metabolism. **Note:** Fold change (FC) represents the ratio of gene expression between two conditions, while FDR (false discovery rate) reflects statistical significance after multiple testing correction. Genes with $|\log_2 FC| > 1$ and FDR < 0.05 were considered significantly differentially expressed. Each dot in the plot represents a gene: colored dots indicate DEGs, and black dots represent non-significant genes.

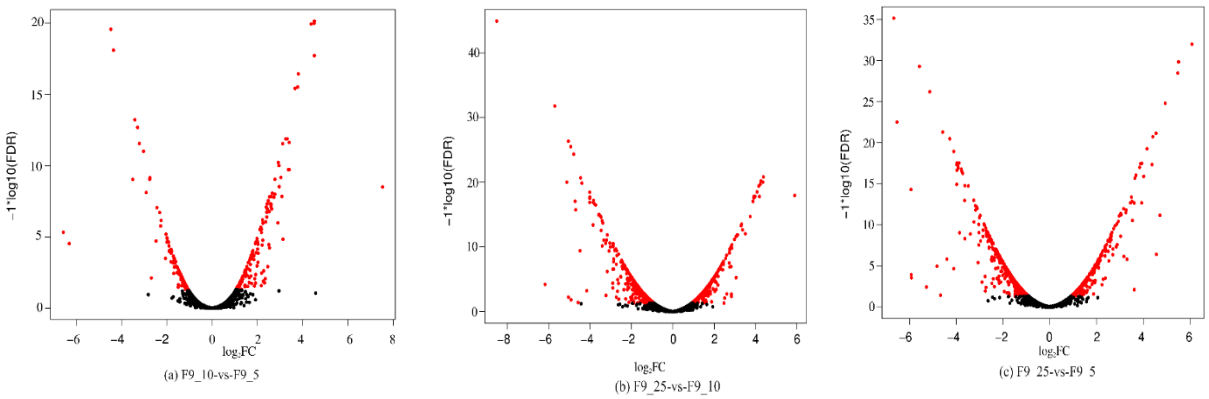

Figure 4. Volcano plots illustrating the distribution of DEGs across the three temperature comparisons.

GO Functional Enrichment Analysis

Gene Ontology (GO) enrichment analysis was conducted using the annotated genome of *Glutamicibacter arilaitensis* Re117 as the reference. Differentially expressed genes (DEGs) identified from transcriptomic comparisons between cultures grown at 5 °C, 10 °C, and 25 °C were analyzed to determine which biological processes and molecular functions were significantly enriched. For each pairwise comparison, the top 20 GO terms with the highest significance were selected for further analysis, and enrichment was assessed using three metrics: enrichment factor, Q-value, and the number of genes enriched in each category. The results revealed that in the comparison between 10 °C and 5 °C (F9_10 vs. F9_5), the upregulated genes were predominantly enriched in the thiamine metabolic process, thiamine biosynthetic process, sulfur compound metabolic process, biotin metabolic process, and biotin biosynthetic process. These results suggest that moderate cold stress at 10 °C stimulates the biosynthesis of essential vitamins and cofactors involved in energy metabolism and cellular stress responses. In the comparison between 25 °C and 10 °C (F9_25 vs. F9_10), upregulated genes were significantly enriched in small molecule metabolic processes, including the metabolism of carboxylic acids, oxoacids, organic acids, cellular amino acids, and organonitrogen compounds.

This finding indicates that cells cultured at ambient temperature reprogram their metabolic activity toward the utilization of a broader range of substrates. In the comparison between 25 °C and 5 °C (F9_25 vs. F9_5), the enrichment pattern overlapped with the F9_25 vs. F9_10 group but also included the histidine metabolic process, suggesting specific metabolic adjustments involving amino acid biosynthesis under extreme cold conditions. The downregulated DEGs showed consistent enrichment patterns across comparisons. In both the F9_25 vs. F9_10 and F9_25 vs. F9_5 groups, significantly enriched GO categories included intrinsic component of membrane, integral component of membrane, membrane, and cellular anatomical entity. These findings imply a shift in membrane composition and structure, likely reflecting adaptations to maintain membrane fluidity and function during cold exposure. In the F9_10 vs. F9_5 group, the most significantly enriched downregulated category was also the intrinsic component of membrane, while endopeptidase activity emerged as the GO category with the highest number of downregulated genes. This pattern suggests a general suppression of proteolytic pathways and stabilization of cellular proteins under colder conditions, which supports energy conservation and maintenance of metabolic balance.

Overall, these enrichment patterns illustrate that *Glutamicibacter arilaitensis* F9 responds to decreasing temperature by enhancing biosynthetic pathways related to cofactor and amino acid production while reducing membrane-associated protein expression and proteolytic activity. The similarity in GO enrichment between the 5 °C and 10 °C groups points to conserved cold-adaptive strategies, whereas the broader metabolic reprogramming observed at 25 °C reflects a distinct physiological shift toward mesophilic growth behavior. The detailed GO enrichment scatter plots for upregulated and downregulated DEGs are presented in Supplementary Figures 1 and 2, respectively.

KEGG Pathway Enrichment Analysis

A KEGG pathway enrichment analysis was conducted to investigate the functional roles of differentially expressed genes (DEGs) in *Glutamicibacter arilaitensis* F9 under varying cultivation temperatures. The top 20 significantly enriched pathways were visualized using a KEGG enrichment scatter plot (Supplementary Figure 3). In this plot, enrichment intensity is indicated by a color gradient ranging from green to red, with larger circle sizes and proximity to the origin representing higher statistical significance.

In the F9_10 vs. F9_5 comparison, DEGs were primarily enriched in pathways such as fatty acid degradation, tryptophan metabolism, the two-component system, and pyruvate metabolism. These enrichments suggest specific transcriptional responses to moderate cold stress (from 10 °C to 5 °C), reflecting adjustments in energy metabolism and environmental sensing. In the F9_25 vs. F9_10 group, significant enrichment was observed in butanoate metabolism, glyoxylate and dicarboxylate metabolism, ABC transporters, and the two-component system, indicating enhanced metabolic versatility under warmer conditions (25 °C). The F9_25 vs. F9_5 comparison group showed pronounced enrichment in the two-component system, pyruvate metabolism, glyoxylate and dicarboxylate metabolism, and butanoate metabolism.

The recurrence of these pathways across multiple comparisons underscores their likely involvement in temperature-dependent adaptation mechanisms. These results collectively highlight that *G. arilaitensis* F9 exhibits coordinated metabolic reprogramming to maintain homeostasis and functionality across a broad thermal range.

Main Enriched Metabolic Pathway Analysis

The two-component system emerged as a consistently enriched metabolic pathway across all three comparison groups (F9_10 vs. F9_5, F9_25 vs. F9_10, and F9_25 vs. F9_5). Notably, temperature reduction induced distinct patterns of differential gene expression. Upregulated genes included the phosphotransferase system component for starch utilization (*PstS*), DNA replication origin recognition and initiation protein A (*DnaA*), glutamine synthetase (*GlnA*), and exopolysaccharide synthesis determinant D (*EpsD*). In contrast, genes such as citrate permease (*TctA*), citrate transport ATP-binding cassette (*TctB*), citrate transport accessory protein (*TctC*), cellulose synthase A (*CtaA*), and 11 other gene products were significantly downregulated. Glyoxylate and dicarboxylate metabolism showed significant enrichment in both the F9_25 vs. F9_10 and F9_25 vs. F9_5 groups.

A temperature downshift from 25°C to 10°C triggered the upregulation of key metabolic enzymes including glutamine synthetase (EC 6.3.1.2), glycine dehydrogenase (EC 1.4.1.27), and glycerol-2-phosphate kinase (EC 2.7.1.165). Meanwhile, enzymes such as catalase (EC 1.11.1.6) and the 2-oxoglutarate metabolic enzyme (EC 2.2.1.5) were downregulated in response to the cold stress.

Fatty acid biosynthesis was prominently enriched in the F9_25 vs. F9_10 group. This enrichment reflected a typical cold stress response, marked by the upregulation of essential biosynthetic enzymes including acetyl-CoA carboxylase (EC 6.4.1.2) and 3-oxoacyl-[acyl-carrier-protein] synthase III (EC 2.3.1.180).

The ABC transporter system also exhibited significant differential expression in the F9_25 vs. F9_10 group. The temperature reduction from 25°C to 10°C led to the upregulation of genes such as sucrose permease (*SsuA*), sucrose transport ATP-binding cassette (*SsuC*), and phosphotransferase system component for starch utilization (*PstS*), along with 13 additional transport-related genes. In contrast, genes encoding the sucrose transport ATP-binding cassette B subunit (*SsuB*), oleate permease complex B subunit (*OpuBC*), oleate permease ATP-binding cassette B subunit (*OpuBB*), and 14 other transporter components were downregulated under cold stress.

Discussion and Conclusion

Differential expression gene analysis

The transcriptomic profiling of *Glutamicibacter arilaitensis* strain F9, a cold-adapted cellulolytic bacterium, was performed under three temperature conditions (5℃, 10℃, and 25℃). A standardized bioinformatics workflow utilizing SOAPnuke, SOAP2, and edgeR was established for comprehensive data processing. During the cold shock response [8], the F9_25-vs-F9_10 comparison group exhibited 731 differentially expressed genes (DEGs). When cultured at 25℃ and subjected to a 15℃ temperature drop to 10℃, 307 genes were upregulated while 424 were downregulated. This pattern of genome-wide transcriptional reprogramming aligns with previous findings by Chen et al. [9–11], demonstrating that strain F9 achieves rapid cold acclimation through large-scale gene expression modulation to enter the cold growth phase within a short timeframe. To adapt to temperature decreases, strain F9 undergoes structural and metabolic adaptations driving the generation of DEGs. Notably, the large temperature gradient (15℃ drop) induces genome-wide transcriptional reprogramming, resulting in significantly higher DEG counts compared to smaller temperature shifts. When cultured at 10℃ and further cooled to 5℃, F9 underwent secondary structural and metabolic adaptations to environmental changes. The F9_10-vs-F9_5 comparison identified 265 DEGs, comprising 123 overlapping genes with the F9_25-vs-F9_10 group and 142 unique DEGs specific to this temperature gradient. The reduced temperature difference (5℃) resulted in moderate transcriptional changes, consistent with the observation that smaller thermal shifts elicit less dramatic genomic responses [3], [14]. Venn diagram analysis revealed 65 conserved DEGs across all three comparison groups. These genes exhibited stepwise expression modulation during temperature decrement, with transcriptional levels dynamically adjusted as culture temperature progressively decreased from 25℃ to 5℃.

This pattern of coordinated gene expression regulation strongly suggests these 65 DEGs are directly implicated in F9's cold adaptability [1], [7].

GO functional enrichment analysis

GO functional enrichment analysis identified biological processes and molecular functions associated with DEGs across the three temperature conditions. The DEGs were predominantly involved in three functional categories: cellular energy metabolism, amino acid biosynthesis, and membrane composition. Significantly upregulated DEGs were enriched in thiamine metabolic process, sulfur compound metabolic process, carboxylic acid metabolic process, small molecule metabolic process, oxoacid metabolic process, biotin metabolic process, and organic acid metabolic process. These interconnected processes suggest F9 enhances its energy production capacity through metabolic pathway optimization to support vital cellular activities under cold stress conditions [3], [14]. Under cold stress, genes involved in thiamine and biotin biosynthesis showed significant upregulation, enhancing bacterial biosynthetic activity. Moreover, upregulated DEGs involved in protein synthesis metabolism were enriched in histidine biosynthetic process, cellular amino acid metabolic process, and organonitrogen compound catabolic process, whichcollectively contribute to amino acid synthesis essential for producing proteins, enzymes, and other nitrogen-containing biomolecules [21], [22]. Conversely, genes associated with endopeptidase activity were downregulated, potentially reducing protein degradation through hydrolysis of peptide chains. Under cold stress, F9 enhances anabolic metabolism of proteins, enzymes, and nitrogenous biomolecules to provide the essential material basis for maintaining cellular homeostasis. This adaptive response is achieved through strategic modulation of gene expression, compensating for reduced enzymatic activity and decreased efficiency of functional proteins at low temperatures [13], [14].

The fluidity of the cell membrane, critical for information exchange and material transport with the environment, is indispensable for normal cellular functions. Psychrophiles employ multiple strategies to regulate membrane fluidity under cold stress, including increasing polyunsaturated fatty acid (PUFA) content, modifying fatty acid saturation ratios, reducing fatty acid polarity via hydroxylation, and inducing trans-to-cis isomerization of double bonds [12–14]. Lauro et al. [12], Cacace et al. [13], and De Maayer et al. [14] demonstrated via transcriptomic and physiological studies that cold stress induces upregulation of membrane synthesis-related genes (fatty acid synthases, phospholipid glycerol transferases, peptidoglycan synthases, and glycosyltransferases) and membrane transport proteins, enhancing membrane integrity to counteract cold-induced fluidity loss and ensure survival under hypothermal conditions.

This study's results align with previous findings showing significantly downregulated DEGs across the three comparison groups (F9_10-vs-F9_5, F9_25-vs-F9_5, and F9_25-vs-F9_10) were enriched in membrane-related GO subcategories including intrinsic and integral components of the membrane. This suggests that under cold conditions, F9 compensates by expanding membrane surface area, modifying membrane lipid composition, and increasing unsaturated fatty acid levels to mitigate transport velocity reduction and metabolic depression [14], [21].

Main enriched metabolic pathway analysis

Two-component system

The two-component system (TCS), a ubiquitous microbial signaling pathway, plays a pivotal role in environmental sensing and metabolic adaptation. Multiple cold-adaptive TCSs have been identified in diverse microorganisms: LisK/LisR in *Listeria monocytogenes* [15], RpfC/RpfG in *Stenotrophomonas maltophilia* [16], DesK/DesR in *Bacillus subtilis* [17], CasK/CasR in psychrotolerant *Bacillus* [18], CB02306/CBO2307 in *Clostridium botulinum* [19], and CheA/CheY in *Yersinia pseudotuberculosis* [20]. These systems are critical for restoring membrane fluidity under cold stress by modulating lipid composition and membrane dynamics. F9 harbors 109 TCS genes, with 97 assigned to 10 known families (e.g., OmpR, Sporulation, CitB) and 12 uncharacterized. Notably, 13 TCS-regulated operon genes showed significant expression differences at 10°C vs. 25°C. The SenX3/RegX3 system (OmpR family) regulates the *pst* operon with *pstS* significantly upregulated, enhancing phosphate transport which is vital for phospholipid biosynthesis and membrane fluidity maintenance under cold stress [14], [19].

The MtrB/MtrA system regulates *dnaA* gene expression, with increased *dnaA* facilitating DNA replication origin recognition, essential for genetic duplication under low temperatures. The GlnL/GlnG system regulates *glnA* expression, increasing glutamine synthetase activity and glutamine production to support protein synthesis and counteract cold-induced protein degradation, thus maintaining cellular homeostasis [14].

Glyoxylate and dicarboxylate metabolism

Gluconeogenesis converts non-carbohydrate precursors such as lactic acid, glycerol, and glucogenic amino acids into glucose or glycogen. Alanine, aspartate, and glutamate undergo transamination to form TCA cycle intermediates (pyruvate, oxaloacetate, α-ketoglutarate) that produce ATP and reducing equivalents sustaining energy homeostasis [3]. In F9, glutamine synthetase (EC 6.3.1.2) and glycine dehydrogenase (EC 1.4.1.27) were significantly upregulated, enhancing glucogenic amino acid catabolism and glucose synthesis. Upregulated glyceraldehyde-3-phosphate kinase (EC 2.7.1.165) and pyruvate carboxylase (EC 6.4.1.3) increased glycolysis/gluconeogenesis flux and TCA cycle intermediates, counteracting cold-induced metabolic stress [21], [22]. Soluble sugars like glucose, sucrose, and fructose accumulate intracellularly as osmolytes under cold stress, increasing osmotic pressure to counteract membrane rigidification and metabolic slowdown. Wang et al. [21] showed Antarctic diatoms accumulate proline and soluble sugars under cold stress. Similarly, Li et al. [22] described trehalose accumulation in fungi with cryoprotective roles. F9's enhanced glucose production suggests glucose acts both as energy substrate and osmotic regulator to maintain membrane integrity and cellular function under cold stress.

Hydrogen peroxide (H_2O_2), a critical signaling molecule, accumulates endogenously under stress, enhancing cold tolerance in plants like tobacco, rapeseed, and Sedum [23–25]. In F9, catalase (EC 1.11.1.6) downregulation likely causes H_2O_2 accumulation, suggesting a role for endogenous H_2O_2 signaling in cold tolerance and ROS balance

Fatty acid biosynthesis

Fatty acid synthases (FAS) types I and II exist in F9. Upregulated acetyl-CoA carboxylase (EC 6.4.1.2) in the Type I system increases malonyl-CoA, the two-carbon donor for fatty acid elongation. Upregulated FabH (EC 2.3.1.180) in the Type II system boosts 3-oxoacyl-[acyl-carrier-protein] production. This dual enzyme upregulation ensures abundant precursors for fatty acid biosynthesis, essential for membrane lipid remodeling and energy homeostasis under cold stress [12], [14].

ABC transporter system

ABC transporters are membrane-bound ATPases mediating substrate transport essential for nutrient uptake and stress adaptation. Under 10℃ vs. 25℃, alkyl sulfate transporters (SsuA, SsuC) were upregulated, while SsuB was downregulated. Osmolyte transporters OpuBC/B showed reduced expression, balancing membrane stability and transport efficiency. Upregulated phosphate transporter PstS and amino acid transporters (GluA-C, TcyC) enhance glutathione precursor supply, while downregulated glutamine transporter GlnH reduces feedback inhibition on glutamate-to-glutamine conversion. Oligopeptide transporter subunits OppA, OppB, OppC, and OppF were upregulated, enhancing oligopeptide transport, while glutathione transporter subunits GsiB-D were similarly upregulated, likely strengthening oxidative stress defenses. Downregulation of nucleotide efflux transporters (BmpA, NupB, NupC) reduces nucleotide loss, preserving intracellular pools [14], [19].

Overall, F9 dynamically regulates ABC transporters to maintain substrate availability for metabolism and antioxidative defense under cold stress, facilitating survival and growth.

Conflict of Interests

The authors declare no conflict of interests.

Authors' contribution

CG. Xu designed the study, performed data analysis and interpretation, and prepared the manuscript. L. X. Yang contributed to experimental design, data analysis, and manuscript revision. J. C. Wang and Y. J. Ma conducted laboratory work and drafted the GO and KEGG enrichment analysis sections, respectively. B. L. Yu contributed to the KEGG pathway analysis. All authors read and approved the final manuscript.

Acknowledgment

This work was supported by the Hulunbuir Science and Technology Plan Project of Inner Mongolia (Grant No. SF2022005). The authors express their gratitude to the College of Agriculture at Hulunbuir University for providing research facilities and an enabling academic environment. Special thanks are extended to Senior Lab Master LI Yan and the technical staff of the Microbiology Laboratory for their support in culture preservation. Appreciation is also extended to Yang Lixia and Shan Dan for their valuable assistance during data collection and analysis.

References:

[1] R. Y. Morita, "Psychrophilic bacteria," *Bacteriol. Rev.*, vol. 39, no. 2, pp. 144–167, 1975. http://doi.org/10.1128/br.39.2.144-167.1975

[2] R. Margesin and V. Miteva, "Diversity and ecology of psychrophilic microorganisms," *Res. Microbiol.*, vol. 162, no. 3, pp. 346–361, 2011. http://doi.org/10.1016/j.resmic.2010.12.004

[3] A. Ramón *et al.*, "A general overview of the multifactorial adaptation to cold: biochemical mechanisms and strategies," *Braz. J. Microbiol.*, vol. 54, no. 3, pp. 2259–2287, 2023. http://doi.org/10.1007/s42770-023-01057-4

[4] S. Y. Zhang *et al.*, "Research progress and applications on mechanisms of cold adaptation in psychrophilic bacteria," *Shandong Chem. Ind.*, vol. 46, no. 17, pp. 63–65+69, 2017.

[5] X. Y. Li, "Research on the cold-adaptation mechanism of β-Glycosidase from *Pseudomonas putida*," M.S. thesis, Dali Univ., Dali, 2023.

[6] G. J. Hu, "Comparative analysis of structural parameters of temperature-adaptive enzymes," M.S. thesis, Yunnan Univ., Kunming, 2022.

[7] R. Cavicchioli, "On the concept of a psychrophile," *ISME J.*, vol. 10, no. 4, pp. 793–795, 2016. http://doi.org/10.1038/ismej.2015.160

[8] G. Horn *et al.*, "Structure and function of bacterial cold shock proteins," *Cell. Mol. Life Sci.*, vol. 64, no. 12, pp. 1457–1470, 2007. http://doi.org/10.1007/s00018-007-6388-4

[9] Z. J. Chen *et al.*, "The genome and transcriptome of a newly described psychrophilic archaeon, *Methanolobus psychrophilus* R15, reveal its cold adaptive characteristics," *Environ. Microbiol. Rep.*, vol. 4, no. 6, pp. 633–641, 2012. http://doi.org/10.1111/j.1758-2229.2012.00389.x

[10] H. C. Gao *et al.*, "Global transcriptome analysis of the heat shock response of *Shewanella oneidensis*," *J. Mycobact.*, vol. 186, no. 22, pp. 7796–7803, 2004. http://doi.org/10.1128/JB.186.22.7796-7803.2004

[11] S. Frank *et al.*, "Functional genomics of the initial phase of cold adaptation of *Pseudomonas putida* KT2440," *FEMS Microbiol. Lett.*, vol. 318, no. 1, pp. 47–54, 2011. http://doi.org/10.1111/j.1574-6968.2011.02237.x

[12] F. M. Lauro *et al.*, "Large-scale transposon mutagenesis of *Photobacterium profundum* SS9 reveals new genetic loci important for growth at low temperature and high pressure," *J. Mycobact.*, vol. 190, no. 5, pp. 1699–1709, 2008. http://doi.org/10.1128/JB.01176-07

[13] G. Cacace *et al.*, "Proteomics for the elucidation of cold adaptation mechanisms in *Listeria monocytogenes*," *J. Proteomics*, vol. 73, no. 10, pp. 2021–2030, 2010. http://doi.org/10.1016/j.jprot.2010.06.011

[14] P. De Maayer *et al.*, "Some like it cold: understanding the survival strategies of psychrophiles," *EMBO Rep.*, vol. 15, no. 5, pp. 508–517, 2014. http://doi.org/10.1002/embr.201338170

[15] G. J. Wang, "Mechanisms of LisK/R two-component system in regulating flagellar gene expression to affect *Listeria monocytogenes* low-temperature growth," M.S. thesis, Huazhong Agric. Univ., Wuhan, 2022.

[16] Q. Wang *et al.*, "Integration of DSF and temperature signals for RpfC/RpfG two-component system modulating protease production in *Stenotrophomonas maltophilia* FF11," *Curr. Microbiol.*, vol. 79, no. 2, p. 54, 2022. http://doi.org/10.1007/s00284-021-02731-2

[17] P. S. Aguilar *et al.*, "Molecular basis of thermosensing: a two-component signal transduction thermometer in *Bacillus subtilis*," *EMBO J.*, vol. 20, no. 7, pp. 1681–1691, 2001. http://doi.org/10.1093/emboj/20.7.1681

[18] S. E. Diomand *et al.*, "The CasKR two-component system is required for the growth of mesophilic and psychrotolerant *Bacillus cereus* strains at low temperatures," *Appl. Environ. Microbiol.*, vol. 80, no. 8, pp. 2493–2503, 2014. http://doi.org/10.1128/AEM.00090-14

[19] Y. Derman *et al.*, "The two-component system CBO2306/CBO2307 is important for cold adaptation of *Clostridium botulinum* ATCC3502," *Int. J. Food Microbiol.*, vol. 167, no. 1, pp. 87–91, 2013. http://doi.org/10.1016/j.ijfoodmicro.2013.06.004

[20] E. Palonen *et al.*, "Expression of signal transduction system encoding genes of *Yersinia pseudotuberculosis* IP32953 at 28 °C and 3 °C," *PLoS One*, vol. 6, no. 9, p. e25063, 2011. http://doi.org/10.1371/journal.pone.0025063

[21] Y. B. Wang *et al.*, "Roles of proline and soluble sugars in the cold adaptation mechanisms of Antarctic diatoms," *Biotechnol. Bull.*, vol. 32, no. 2, pp. 198–202, 2016.

[22] Y. P. Li *et al.*, "Trehalose in fungi and its functions under cold stress," *J. Edible Fungi*, vol. 20, no. 4, pp. 71–77, 2013.

[23] Z. Q. Shen *et al.*, "Effects of exogenous EBR and H_2O_2 spray on cold stress resistance in tobacco seedlings," *J. Yunnan Agric. Univ. (Nat. Sci.)*, vol. 37, no. 4, pp. 623–629, 2022.

[24] L. X. Hou, "H_2O_2 impacts on physiological indices of rape seedlings under low temperatures," *Hubei Agric. Sci.*, vol. 52, no. 21, pp. 5144–5146+5152, 2013.

[25] Q. J. Lai *et al.*, "Exogenous H_2O_2 pretreatment enhances cold resistance and improves yield and quality of *Sedum adolphii*," *Chin. Mater. Med.*, vol. 53, no. 21, pp. 6874–6880, 2022.

Supplementary materials

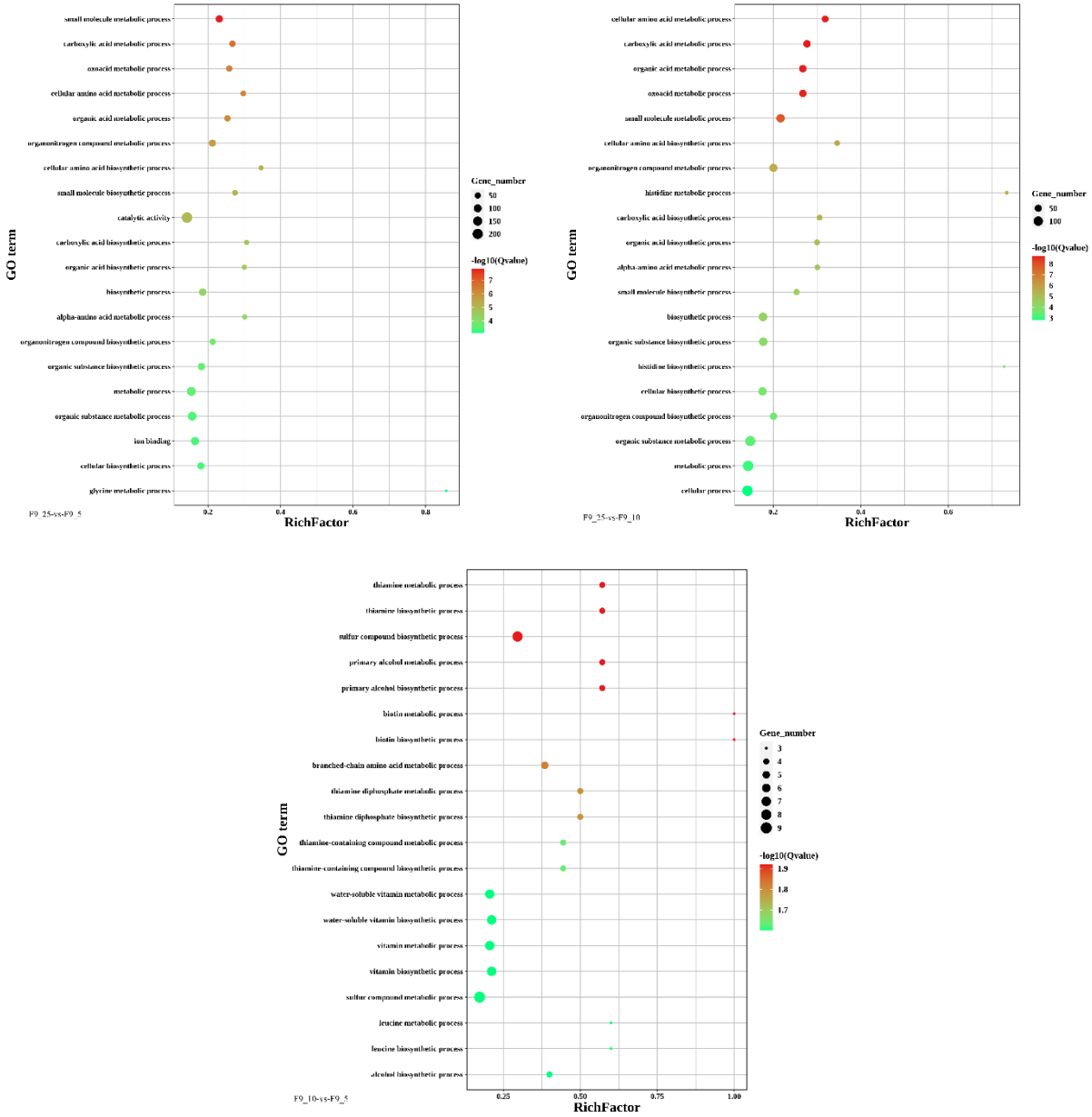

Figure 1. Up-regulated gene GO enrichment scatter plot

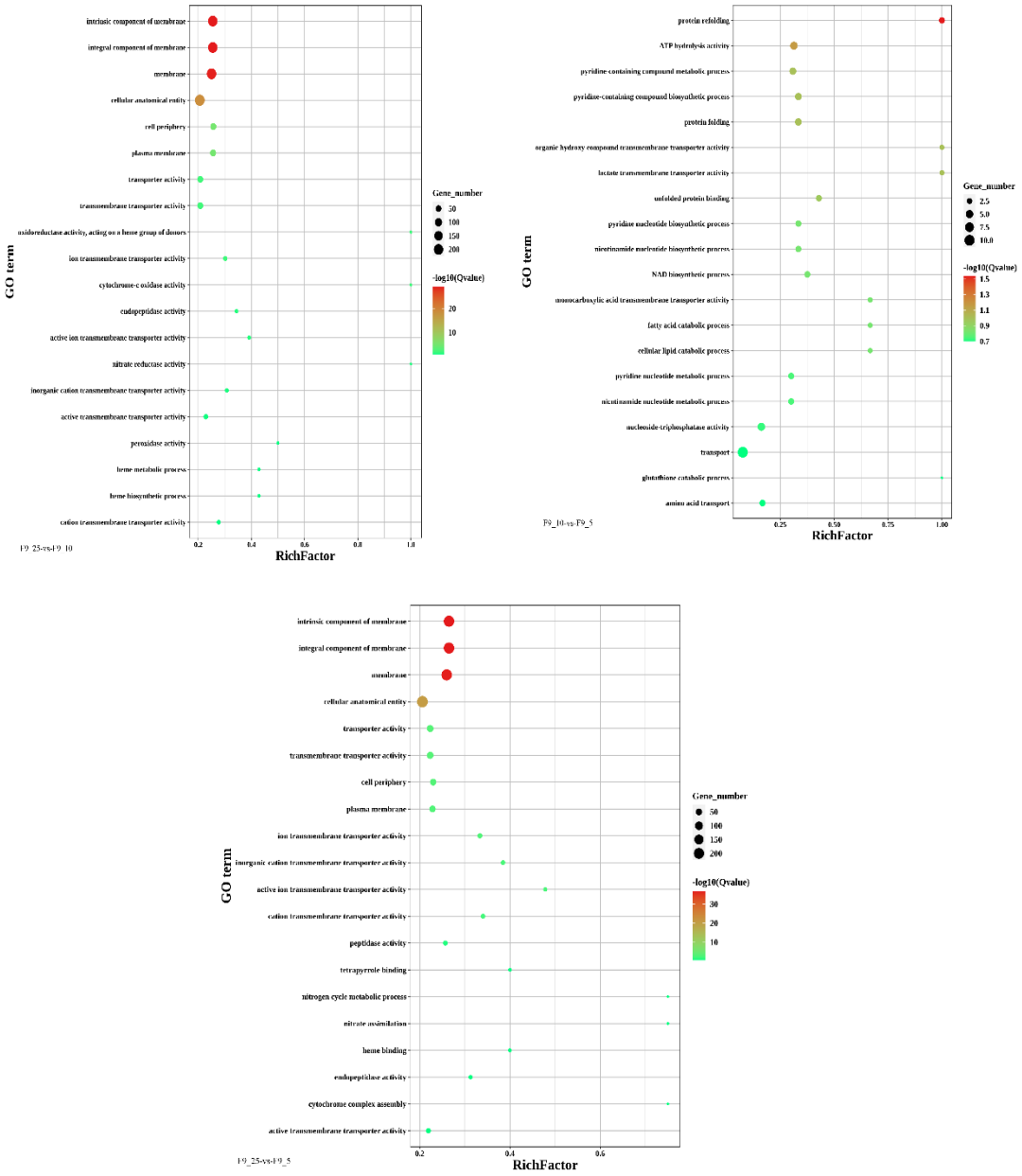

Figure 2. Down-regulated gene GO enrichment scatter plot

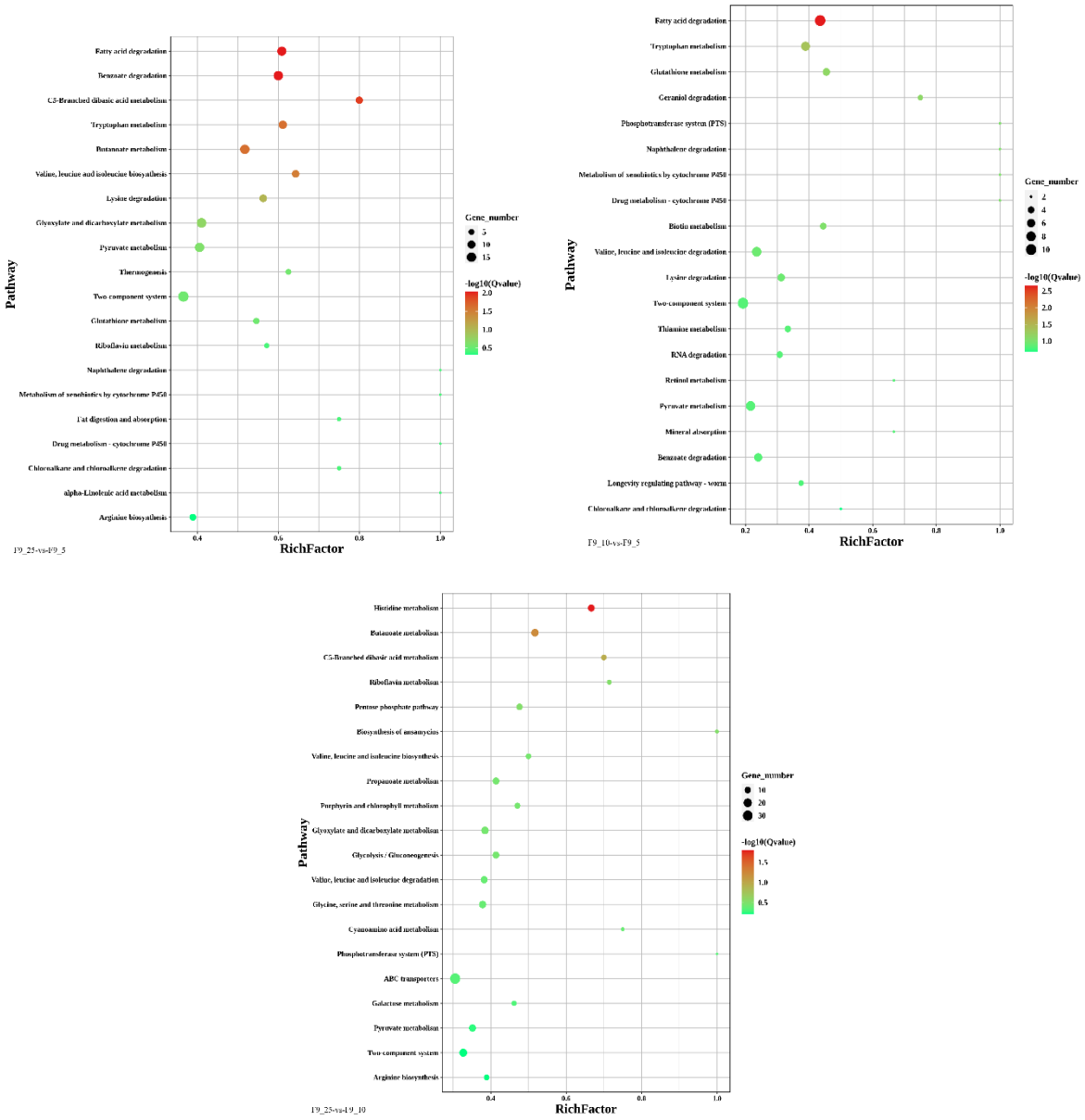

Figure 3. KEGG enrichment scatter plot of differentially expressed genes